

Glaucoma discrimination of segmented cirrus spectral domain optical coherence tomography (SD-OCT) macular scans

Jacek Kotowski,¹ Lindsey S Folio,^{1,2} Gadi Wollstein,¹ Hiroshi Ishikawa,^{1,2} Yun Ling,^{1,3} Richard A Bilonick,^{1,3} Larry Kagemann,^{1,2} Joel S Schuman^{1,2}

► Additional data are published online only. To view these files please visit the journal online (<http://dx.doi.org/10.1136/bjophthalmol-2011-301021>).

¹Department of Ophthalmology, UPMC Eye Center, Eye and Ear Institute, Ophthalmology and Visual Science Research Center, University of Pittsburgh School of Medicine, Pittsburgh, Pennsylvania, USA

²Department of Bioengineering, Swanson School of Engineering, University of Pittsburgh, Pittsburgh, Pennsylvania, USA

³Department of Biostatistics, Graduate School of Public Health, University of Pittsburgh, Pittsburgh, Pennsylvania, USA

Correspondence to

Dr Gadi Wollstein, 203 Lothrop Street, Suite 834.1, Pittsburgh, PA 15213, USA; wollsteing@upmc.edu
Published Online First
22 August 2012

ABSTRACT

Aims To evaluate the glaucoma discriminating ability of macular retinal layers as measured by spectral domain optical coherence tomography (SD-OCT).

Methods Healthy, glaucoma suspect and glaucomatous subjects had a comprehensive ocular examination, visual field testing and SD-OCT imaging (Cirrus HD-OCT; Carl Zeiss Meditec, Dublin, California, USA) in the macular and optic nerve head regions. OCT macular scans were segmented into macular nerve fibre layer (mNFL), ganglion cell layer with inner plexiform layer (GCIP), ganglion cell complex (GCC) (composed of mNFL and GCIP), outer retinal complex and total retina. Glaucoma discriminating ability was assessed using the area under the receiver operator characteristic curve (AUC) for all macular parameters and mean circumpapillary retinal nerve fibre layer (cpRNFL).

Results Analysis was performed on 51 healthy, 49 glaucoma suspect and 63 glaucomatous eyes. The median visual field MD was -2.21 dB (IQR: -6.92 to -0.35) for the glaucoma group, -0.32 dB (IQR: -1.22 to 0.73) for the suspect group and -0.18 dB (IQR: -0.92 to 0.71) for the healthy group. Highest age adjusted AUCs were found for average GCC and GCIP (AUC=0.901 and 0.900, respectively) and their sectoral measurements: infero-temporal (0.922 and 0.913), inferior (0.904 and 0.912) and supero-temporal (0.910 and 0.897). These values were similar to the discriminating ability of the mean cpRNFL (AUC=0.913). Comparison of these AUCs did not yield any statistically significant difference (all $p>0.05$).

Conclusions SD-OCT GCIP and GCC measurements showed similar glaucoma diagnostic ability and were comparable with that of cpRNFL.

INTRODUCTION

Glaucoma is an optic neuropathy characterised by irreversible damage to the retinal ganglion cells (RGCs), retinal nerve fibre layer (RNFL) and optic nerve head, accompanied with visual field (VF) loss and possible blindness. As appropriate treatment can slow disease progression and preserve vision, the ability to diagnose glaucoma early and detect its progression is therefore a very important aspect of disease management.

Macular ganglion cells constitute approximately 50% of all RGCs.¹ In contrast to the peripheral retina where the ganglion cell layer is only one cell thick, there are up to seven layers of RGC bodies in the macula. The primary pathology of glaucoma involves the loss of ganglion cells and the RGC density is the highest within the macula.

Therefore, any such loss should theoretically be easiest to detect in the macular region, making evaluation of this region useful in the diagnosis of glaucoma.² Several studies demonstrated that the total retinal thickness is a good surrogate for glaucomatous ganglion cell layer damage as measured by time domain optical coherence tomography (TD-OCT).²⁻⁸ However, even though total macular thickness was found to be significantly associated with glaucoma, its diagnostic ability was significantly worse than that of circumpapillary (cp) RNFL thickness.⁸⁻¹² The lower discriminating power of the macular measurements could be related to the fact that the retinal layers affected by glaucoma constitute only a third of the total macular thickness. The remaining two-thirds that are not affected by glaucoma might contribute to measurement variability due to confounding effects caused by non-glaucomatous macular pathologies such as diabetes or macular degeneration. It is also possible that the decreased discriminating power of total macular thickness measurements is caused by undersampling of the affected tissue as the macular scan covers only a subpopulation of ganglion cells whereas the cpRNFL scan assesses 100% of ganglion cell axons. To improve the diagnostic ability of the macular measurements, it is desirable to segment the retinal layers to allow for assessment of layers specifically affected by the glaucomatous process. The evaluation of data obtained using segmentation algorithms developed for TD-OCT demonstrated that the glaucoma diagnostic ability of the four innermost retinal layers was significantly higher than the diagnostic ability of the total macular thickness and comparable with the diagnostic performance of cpRNFL thickness.¹³ However, the relatively low resolution and scanning speed of TD-OCT resulted in frequent border detection failure in the segmentation of the inner retinal layers.

The technical advances of spectral domain OCT (SD-OCT) addressed many of the limitations of TD-OCT by providing faster scanning and higher resolution. SD-OCT also introduced volumetric three-dimensional macular cube scans, theoretically improving the reliability of macular measurements. Similar to TD-OCT, studies evaluating the diagnostic ability of SD-OCT macular parameters have shown that the thickness of the ganglion cell complex (GCC) composed of three innermost retinal layers (nerve fibre layer (NFL), RGC layer and inner plexiform layer) offered higher diagnostic power than the total macular thickness in

differentiating between perimetric glaucoma and healthy eyes^{14 15} and similar to that of cpRNFL thickness.^{14 16–19} However, the NFL overlying the RGCs in a given region of the macula consists of axons originating from the underlying RGCs and includes axons traversing along the same arcuate path but originating from RGCs located upstream. As a consequence, the NFL or GCC thickness measurement obtained from one retinal location can have poor correspondence with the matching VF location. We hypothesise that excluding the macular (m)NFL from the GCC would improve the structure–function relationship and improve glaucoma diagnostic ability. The purpose of this study was to evaluate the ability of individual retinal layers thickness measurements as obtained by SD-OCT in discriminating between healthy eyes and eyes with early open angle glaucoma.

METHODS

Subjects

Healthy, glaucoma suspect and glaucoma subjects from the Pittsburgh Imaging Technology Trial (PITT) were selected for this observational cross-sectional study. The PITT study is a prospective longitudinal study designed to assess ocular structure over time carried out at the University of Pittsburgh Medical Center Eye Center. The study was approved by the institutional review board and ethics committee and informed consent was obtained from all subjects. This study followed the tenets of the Declaration of Helsinki and was conducted in compliance with the Health Insurance Portability and Accountability Act.

All participants had a comprehensive ocular examination by glaucoma specialists, reliable Swedish Interactive Thresholding Algorithm standard 24-2 perimetry (Humphrey Field Analyzer, Carl Zeiss Meditec (CZM), Dublin, California, USA), and SD-OCT (Cirrus HD-OCT; CZM) scanning of the macular and peripapillary regions at the same visit. Visual acuity was 20/40 or better, refractive error between -6.00 and $+3.00$ D, and no visually significant media opacities were present. Subjects were also excluded from the study if they had a history of diabetes, any macular pathology, conditions affecting VF other than glaucoma, a history of ocular trauma or surgery other than glaucoma interventions or uncomplicated cataract extraction or were on medications known to affect retinal thickness. Qualified VF examinations had less than 30% fixation losses, false-positive or false-negative responses.

The healthy group consisted of subjects with normal findings on ocular exam, no history of elevated intraocular pressure and full VF. Full VF was defined as a mean deviation (MD) and pattern SD (PSD) within 95% limits of the normal population, and VF glaucoma hemifield test within normal limits. Glaucomatous eyes had clinically determined optic disc rim notching, cup asymmetry, large cupping (vertical cup to disc ratio >0.7), RNFL defect or intraocular pressure >21 mm Hg in the presence of reliable and repeatable abnormal VF test results, defined as a PSD outside of the 95% limits of the normal population or glaucoma hemifield test outside normal limits. Glaucoma suspect consisted of individuals with ocular hypertension and/or optic nerve head changes as defined above in the presence of full VF.

SD-OCT

Cirrus HD-OCT (software V5.0) acquires images at a speed of 27 000 A-scans per second and $5\ \mu\text{m}$ axial resolution in tissue. The Macular Cube 200×200 protocol was used to obtain macular thickness measurements. This scan generates a cube of

data by performing raster scanning in a 6×6 mm square grid consisting of 200 frames of horizontal linear B-scans with 200 A-scan lines per B-scan. The Optic Disc Cube 200×200 scan was used to obtain cpRNFL thickness measurements. This scan is similar to the Macular Cube 200×200 scan and RNFL thickness is extracted from a 3.4 mm diameter circle centred on the optic nerve head. Scans with signal strength <7 , motion artefacts (assessed subjectively as a discontinuity of major blood vessels) or scans with segmentation errors were excluded. Thickness data for the macular parameters were obtained using manufacturer's prerelease segmentation software from an elliptical annulus centred on the fovea with an inner vertical radius of 0.5 mm and outer vertical radius of 2 mm, stretched horizontally by 20%. The elliptical annulus was divided into six sectors, each subtending 60° as shown in figure 1.

Data and statistical analysis

Data from the right eye of qualified subjects were used for the analysis. All macular OCT images were automatically segmented into the following layers: mNFL, ganglion cell layer with inner plexiform layer (GCIP), GCC (composed of mNFL and GCIP), outer retinal complex (ORC) (composed of the remaining retinal layers, starting with the inner nuclear layer) and total retina (TR). cpRNFL thickness was calculated by the Cirrus HD-OCT system software.

Differences in thicknesses among healthy, glaucoma suspect and glaucomatous eyes were evaluated using analysis of variance. Area under the receiver operating characteristic curve (AUC) was used to assess the discrimination ability between healthy and glaucomatous eyes (glaucoma suspect eyes not included) for each macular layer globally and in each sector and for cpRNFL thickness. To account for age imbalance between the groups, age was included as a covariate in the model. The jackknife method²⁰ was used to compare AUCs. A secondary analysis was performed to evaluate the ability to differentiate

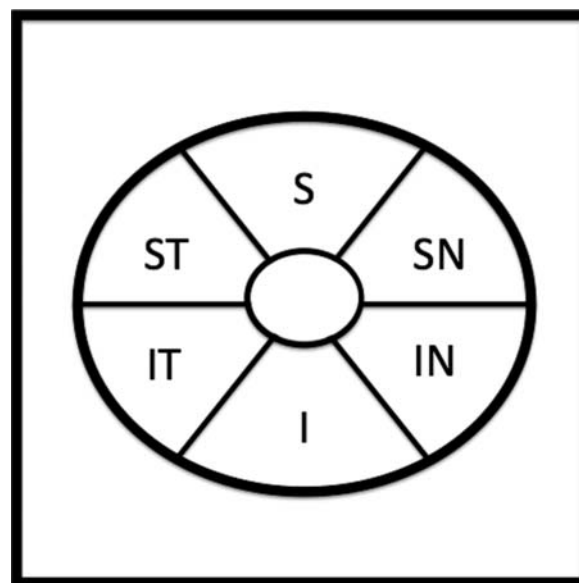


Figure 1 Schematic of the elliptical annulus used for data sampling within the $6\ \text{mm}\times 6\ \text{mm}$ Cirrus HD-OCT Macular Cube 200×200 scan. The annulus has an inner vertical radius of 0.5 mm and an outer vertical radius of 2 mm, stretched horizontally by 20%. I, inferior; IN, infero-nasal; IT, infero-temporal; S, superior; SN, supero-nasal; ST, supero-temporal.

Table 1 Comparison of study population characteristics

	Healthy	Suspect	Glaucoma	p Value
Number of subjects	51	49	63	
Male (%)	37.3	36.7	38.1	0.989*
Age (years)†	54.8 (51.6 to 57.9)	61.6 (58.4 to 64.7)	64.3 (61.5 to 67.1)	<0.0001‡
Visual field MD (dB)§	−0.18 (−0.92 to 0.71)	−0.32 (−1.22 to 0.73)	−2.21 (−6.92 to −0.35)	<0.0001¶
Visual field PSD (dB)§	1.48 (1.3 to 1.69)	1.55 (1.32 to 1.73)	2.99 (1.65 to 8.84)	<0.0001¶

* χ^2 Test.

†Mean (95% CI).

‡Analysis of variance.

§Median (IQR).

¶Wilcoxon/Kruskal–Wallis tests (Rank Sums).

dB, decibels; MD, mean deviation; PSD, pattern SD.

healthy eyes from non-healthy eyes (glaucomatous and glaucoma suspect eyes combined into one group).

Statistical analysis was performed using JMP 8 (SAS Institute, Cary, North Carolina, USA) and R Language and Environment for Statistical Computing program (version 2.13.0; see <http://www.R-project.org>).²¹ A p value < 0.05 was considered as statistically significant.

RESULTS

In all, 166 eyes were evaluated for this study. Three eyes were excluded due to failure of the segmentation algorithm. Analysis was performed on 163 right eyes of 63 glaucoma patients, 49 glaucoma suspect and 51 healthy subjects. The demographic and clinical information for each group is summarised in table 1. Statistically significant differences were found between the groups for age, MD and PSD.

Table 2 and online supplementary table S1A summarise the global and sectoral thickness measurements for each layer by clinical group. mNFL thickness, GCIP, GCC, TR, and cpRNFL thickness were the highest in the healthy group, followed by the suspect group and lowest in the glaucoma group. The differences were all statistically significant. No statistically significant differences between the groups were observed for any of the ORC parameters. Figures 2 and 3 show an example of the GCC and GCIP map for a healthy and glaucomatous eye, respectively.

Assessing the discriminating ability of macular OCT measurements between healthy subjects and subjects with perimetric glaucoma (table 3 and online supplementary table S2A), GCC and GCIP had the highest AUCs that were statistically significantly higher than the AUCs for average TR (p=0.020 and 0.016) and average ORC (<0.001 for both). The AUC for average GCC was significantly higher than the AUC for average

mNFL (p=0.023). No other difference between pairs of AUCs for global OCT parameters was statistically significant. Mean cpRNFL had similar discrimination ability as GCC and GCIP and significantly better discrimination than TR, ORC and mNFL. In order to reach a statistically significant difference in the studied population between mean cpRNFL and GCC and GCIP their AUCs should have been below 0.861 and 0.863, respectively. For the global parameters, a preset sensitivity of 95% and 80% had a specificity of 39% and 81%, respectively, for GCC, 54% and 83% for GCIP and 72% and 83% for cpRNFL.

In the secondary analysis, the largest age adjusted AUCs for discriminating between healthy and non-healthy eyes (combination of glaucoma and glaucoma suspect eyes) were found for the infero-temporal (AUC=0.834 and 0.824), inferior (0.823 and 0.822) and supero-temporal (0.830 and 0.823) sectors and average (0.814 and 0.808) GCC and GCIP, respectively (table 3 and online supplementary table S2A). These values were similar to the discrimination ability of mean cpRNFL (AUC=0.818). The difference in AUCs of the global parameters did not reach a statistically significant level for any comparisons except for ORC and GCC (p=0.005) and ORC and GCIP (p=0.005).

DISCUSSION

In the present study, we investigated the glaucoma discriminating capability of Cirrus HD-OCT macular intraretinal thickness measurements. We showed that SD-OCT thickness measurements of the inner retinal layers in the macula have comparable glaucoma diagnostic ability with and without the inclusion of the mNFL and similar to cpRNFL thickness measurements. Both inner retinal macular layers and cpRNFL outperformed the total macular retinal thickness and outer retinal

Table 2 Global retinal thickness measurements (in μ m) reported as mean and 95% CI

Parameter	Healthy	Suspect	Glaucoma	p Value*
mNFL average	32.6 (31.4 to 33.9)	31.7 (30.4 to 33.0)	27.6 (26.5 to 28.8)†‡	<0.0001
GCC average	112.8 (109.8 to 115.7)‡	107.5 (104.5 to 110.5)†	95.5 (92.8 to 98.1)†‡	<0.0001
GCIP average	80.1 (78.1 to 82.2)‡	75.9 (73.8 to 78.0)†	67.8 (66.0 to 69.7)†‡	<0.0001
ORC average	193.2 (190.0 to 196.4)	191.3 (188.5 to 195.6)	192.4 (189.5 to 195.3)	0.715
TR average	305.9 (301.8 to 310.2)‡	298.9 (294.6 to 303.2)†	287.8 (284.0 to 291.7)†‡	<0.0001
Mean cpRNFL	91.5 (88.7 to 94.3)‡	86.6 (83.7 to 89.4)†	72.3 (69.8 to 74.8)†‡	<0.0001

*One way analysis of variance.

†Statistically significant difference from healthy subject (Student t test).

‡Statistically significant difference from suspect subject (Student t test).

cpRNFL, circumferential retinal nerve fibre layer; GCC, ganglion cell complex; GCIP, ganglion cell layer with inner plexiform layer; mNFL, macular nerve fibre layer; ORC, outer retinal complex; TR, total retina.

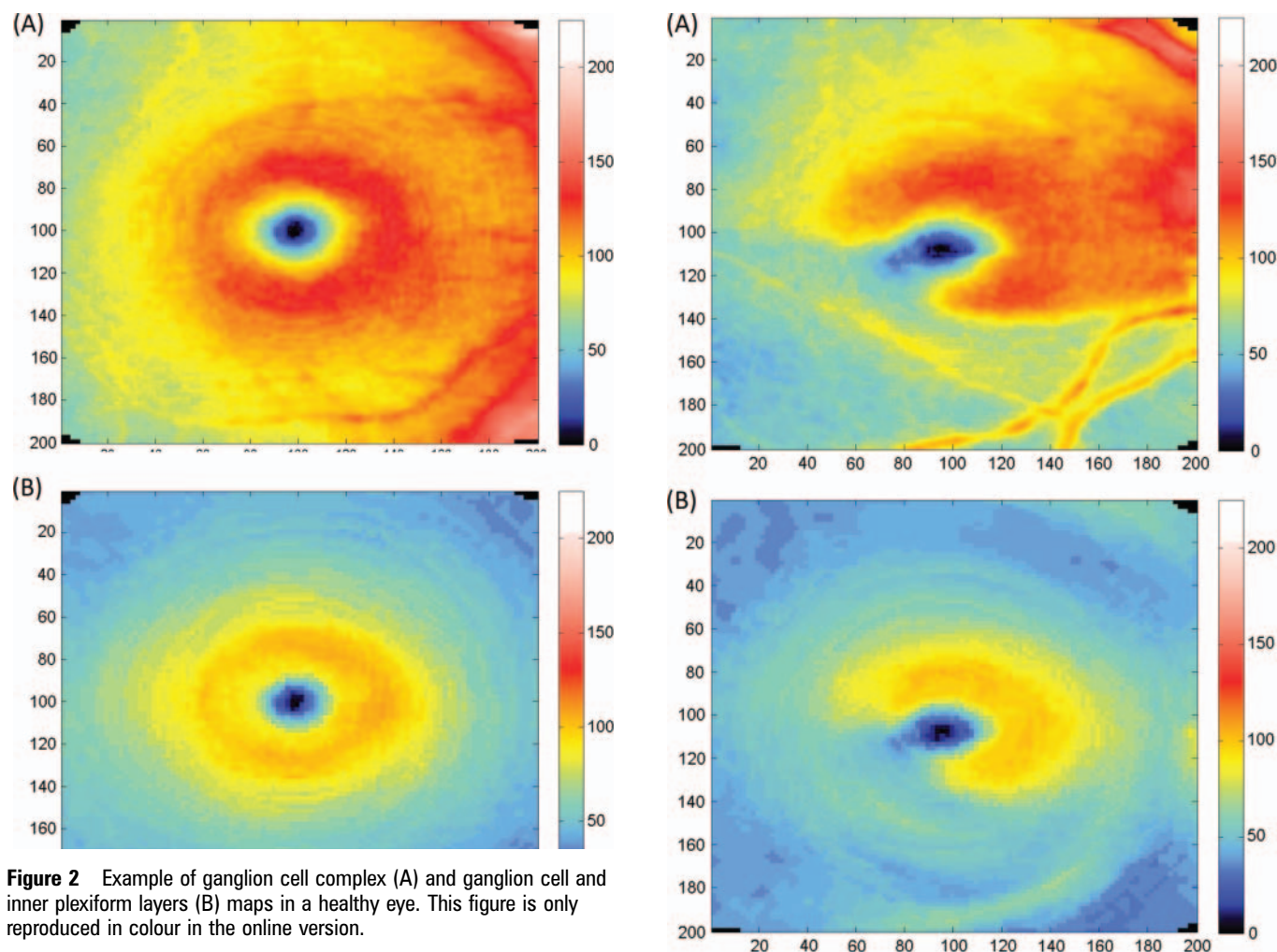


Figure 2 Example of ganglion cell complex (A) and ganglion cell and inner plexiform layers (B) maps in a healthy eye. This figure is only reproduced in colour in the online version.

layer thickness. Prior investigations using TD-OCT have shown that measuring the thickness of the innermost retinal layers in the macula offers higher glaucoma discriminating power than measuring the total retinal thickness.^{13 22} In a study investigating the diagnostic capability of RTVue SD-OCT macular parameters, GCC thickness was found to offer a significantly higher discriminating power ($AUC=0.90$) than total macular thickness as measured by SD-OCT and TD-OCT ($AUC=0.85$ for both SD-OCT and TD-OCT) in differentiating between perimetric glaucoma and healthy eyes.¹⁵ In another study, the AUC for GCC volume in the central 5 mm diameter area of the macula obtained by RTVue SD-OCT was significantly greater than the AUC for the total retinal volume in the same area (0.922 and 0.857, respectively).¹⁴ It has to be noted, however, that in these studies the differences were statistically significant only for subjects with perimetric glaucoma. No statistically significant differences were detected when comparisons were made between healthy eyes and eyes with preperimetric glaucoma. Similar to these studies, significant differences in AUCs between GCC or GCIP and total retinal thickness were shown when analysing healthy and glaucomatous eyes only. However, in the secondary analysis, the improved performance of GCC and GCIP did not reach a statistically significant level, probably due to the overall early glaucomatous stage of the combined group (glaucoma and glaucoma suspect eyes) as reflected by median VF MD of -0.95 dB. The subject populations evaluated in the studies mentioned above had more advanced disease with mean VF

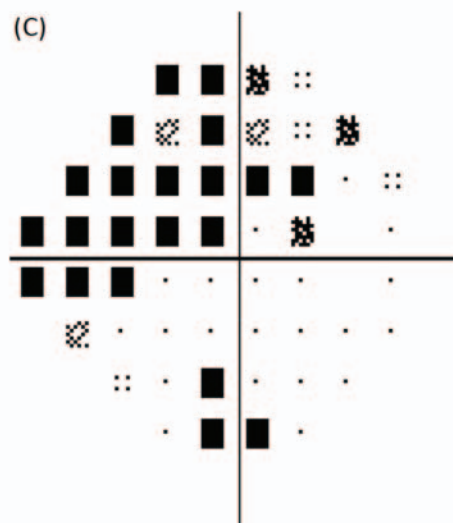


Figure 3 Example of ganglion cell complex (A) and ganglion cell and inner plexiform layers (B) maps in a glaucomatous eye. Thickness reduction is evident in the infero-temporal region corresponding with superior visual field defect (C). This figure is only reproduced in colour in the online version.

MDs of -4.6 and -9.1 dB. We chose to include in our study, as a secondary analysis, the glaucoma suspect eyes in order to evaluate the diagnostic ability of the OCT parameters in a heterogeneous population representative of patients followed in a

Table 3 Age adjusted area under the receiver operating characteristics curve (AUC) for global thickness measurements

Parameter	Healthy versus glaucoma		Healthy versus glaucoma+ suspect	
	AUC	95% CI	AUC	95% CI
mNFL average	0.832	0.757 to 0.907	0.765	0.690 to 0.839
GCC average	0.901	0.843 to 0.959	0.814	0.748 to 0.880
GCIP average	0.900	0.842 to 0.959	0.808	0.742 to 0.875
ORC average	0.730	0.636 to 0.823	0.708	0.626 to 0.790
TR average	0.839	0.765 to 0.913	0.774	0.701 to 0.847
cpRNFL	0.913	0.845 to 0.960	0.818	0.753 to 0.883

cpRNFL, circumpapillary retinal nerve fibre layer; GCC, ganglion cell complex; GCIP, ganglion cell layer with inner plexiform layer; mNFL, macular nerve fibre layer; ORC, outer retinal complex; TR, total retina.

typical academic glaucoma clinic. The inclusion of glaucoma suspect also allowed us to evaluate the diagnostic parameters in subjects in the earliest stages of the disease when a new diagnostic test is most useful. However, we cannot rule out that some of the preperimetric subjects are actual healthy subjects, which leads to the reduced discriminatory ability of the diagnostic parameters.

Consistent with prior investigations, macular parameters in this study had similar discriminating ability for glaucoma diagnosis as mean cpRNFL thickness. It is known that approximately half of the RGCs are located within the macula; however, the remaining peripheral population is also affected by the glaucomatous process. In contrast to the cpRNFL scan, which assesses axons originating from throughout the retina, the macular scan does not assess the peripheral retina. The Cirrus HD-OCT macular scan covers a 6 mm×6 mm square, but the segmentation data were sampled from a smaller elliptical annulus extending up to 2 mm vertically and 2.4 mm horizontally from the fovea. Studies using TD-OCT have shown that glaucomatous damage is most noticeable in the peripheral macular regions, within the 2–3 mm outer ring.^{10–22} Macular volume reduction in glaucomatous eyes was also found to be greater in the peripheral macula in a study using SD-OCT.¹⁴ In that study, the per cent reduction for TR and GCC volume was –1.47 and –5.45 for 1 mm radius, –6.25 and –13.67 for 3 mm radius, and –8.26 and –16.18 for 5 mm radius, respectively. It is thus possible that the discriminating power of the macular measurements in our study could be improved by extending the scan into more peripheral macular regions. Nonetheless, the smaller annulus can provide thickness information even in situations of less than perfectly centred scans thus allowing for better comparison between visits and across wider populations. It should also be noted that since subjects were classified as glaucomatous based on the clinical evaluation of the optic nerve head region and not the macular region, this resulted in a potential selection bias in favour of the cpRNFL. Despite this potential bias, the glaucoma discrimination ability of macular parameters was similar to that of cpRNFL. Our study has shown that the GCC and GCIP thickness measurements in the inferior, infero-temporal and supero-temporal sectors tend to offer the best discriminatory performance. Earlier OCT studies have shown that the inferior and infero-temporal maculae tend to be most susceptible to glaucomatous damage.^{10–14, 16–22, 23} Our results are in agreement with these investigations.

The segmentation software used in this analysis has the unique feature of quantifying the GCIP without including the mNFL (as used by segmentation software available on other

SD-OCT devices) allowing for the evaluation of the diagnostic value of this layer. In our study, the diagnostic performance of GCIP and GCC was comparable. However, the overlap in CI on the AUCs, observed in our study, limits our ability to definitely determine which parameter is better in making the diagnosis. Moreover, due to a relatively small subject population, only large differences between parameters could be expected to reach statistical significance. Because the nerve fibre bundles in a given macular region are composed of axons originating from the underlying ganglion cells in this area and include axons traversing over this area and originating from ganglion cells in other parts of the macula, GCIP measurements might provide better correspondence with localised VF defects. This can potentially increase the strength of the spatial relationship between structure and function and may prove useful in monitoring glaucoma. However, further studies are needed to assess the reproducibility of these measurements before a clear recommendation on the preferred layer for glaucoma discrimination can be made.

In conclusion, Cirrus HD-OCT macular intraretinal parameters offer glaucoma diagnostic ability comparable with that of cpRNFL thickness. The exclusion of the mNFL did not change the diagnostic ability of the inner retinal measurements. The ability of using cpRNFL and/or macula measurements might further enhance the utility of OCT in glaucoma detection.

Acknowledgements This work was supported in part by National Institute of Health grants R01-EY13178, and P30-EY08098 (Bethesda, MD), The Eye and Ear Foundation (Pittsburgh, PA) and an unrestricted grant from Research to Prevent Blindness (New York, NY).

Contributors Design of the study: JK, GW; conduct of the study: JK, LSF; data analysis and interpretation: JK, RAB, YL, GW; manuscript preparation: JK; manuscript review: GW, JSS, LSF, HI, LK; manuscript final approval: JK, GW, JSS.

Funding Supported in part by the National Institute of Health grants R01-EY13178 and P30-EY08098 (Bethesda, MD), The Eye and Ear Foundation (Pittsburgh, PA) and an unrestricted grant from Research to Prevent Blindness (New York, NY).

Competing interests J Kotowski: None. LS Folio: None. G Wollstein: None. L Kagemann: None. H Ishikawa: None. Y Ling: None. RA Bilonick: None. JS Schuman: Royalties for intellectual property licensed by Massachusetts Institute of Technology to Carl Zeiss Meditec.

Patient consent All subjects signed informed consent approved by the University of Pittsburgh Institutional Review Board.

Ethics approval The study was approved by the University of Pittsburgh Institutional Review Board.

Provenance and peer review Not commissioned; externally peer reviewed.

REFERENCES

- Curcio CA, Allen KA. Topography of ganglion cells in human retina. *J Comp Neurol* 1990;**300**:5–25.
- Zeimer R, Asrani S, Zou S, et al. Quantitative detection of glaucomatous damage at the posterior pole by retinal thickness mapping. A pilot study. *Ophthalmology* 1998;**105**:224–31.
- Lederer DE, Schuman JS, Hertzmark E, et al. Analysis of macular volume in normal and glaucomatous eyes using optical coherence tomography. *Am J Ophthalmol* 2003;**135**:838–43.
- Giovannini A, Amato G, Mariotti C. The macular thickness and volume in glaucoma: an analysis in normal and glaucomatous eyes using OCT. *Acta Ophthalmol Scand Suppl* 2002;**236**:34–6.
- Greenfield DS, Bagga H, Knighton RW. Macular thickness changes in glaucomatous optic neuropathy detected using optical coherence tomography. *Arch Ophthalmol* 2003;**121**:41–6.
- Tanito M, Imai N, Ohira A, et al. Reduction of posterior pole retinal thickness in glaucoma detected using the retinal thickness analyzer. *Ophthalmology* 2004;**111**:265–75.
- Wollstein G, Schuman JS, Price LL, et al. Optical coherence tomography (OCT) macular and peripapillary retinal nerve fiber layer measurements and automated visual fields. *Am J Ophthalmol* 2004;**138**:218–25.

8. **Guedes V**, Schuman JS, Hertzmark E, *et al*. Optical coherence tomography measurement of macular and nerve fiber layer thickness in normal and glaucomatous human eyes. *Ophthalmology* 2003;**110**:177–89.
9. **Wollstein G**, Ishikawa H, Wang J, *et al*. Comparison of three optical coherence tomography scanning areas for detection of glaucomatous damage. *Am J Ophthalmol* 2005;**139**:39–43.
10. **Medeiros FA**, Zangwill LM, Bowd C, *et al*. Evaluation of retinal nerve fiber layer, optic nerve head, and macular thickness measurements for glaucoma detection using optical coherence tomography. *Am J Ophthalmol* 2005;**139**:44–55.
11. **Leung CK**, Chan WM, Yung WH, *et al*. Comparison of macular and peripapillary measurements for the detection of glaucoma: an optical coherence tomography study. *Ophthalmology* 2005;**112**:391–400.
12. **Ojima T**, Tanabe T, Hangai M, *et al*. Measurement of retinal nerve fiber layer thickness and macular volume for glaucoma detection using optical coherence tomography. *Jpn J Ophthalmol* 2007;**51**:197–203.
13. **Ishikawa H**, Stein DM, Wollstein G, *et al*. Macular segmentation with optical coherence tomography. *Invest Ophthalmol Vis Sci* 2005;**46**:2012–17.
14. **Mori S**, Hangai M, Sakamoto A, *et al*. Spectral-domain optical coherence tomography measurement of macular volume for diagnosing glaucoma. *J Glaucoma* 2010;**19**:528–34.
15. **Tan O**, Chopra V, Lu AT, *et al*. Detection of macular ganglion cell loss in glaucoma by Fourier-domain optical coherence tomography. *Ophthalmology* 2009;**116**:2305–14e1–2.
16. **Nakatani Y**, Higashide T, Ohkubo S, *et al*. Evaluation of macular thickness and peripapillary retinal nerve fiber layer thickness for detection of early glaucoma using spectral domain optical coherence tomography. *J Glaucoma* 2011;**20**:252–9.
17. **Seong M**, Sung KR, Choi EH, *et al*. Macular and peripapillary retinal nerve fiber layer measurements by spectral domain optical coherence tomography in normal-tension glaucoma. *Invest Ophthalmol Vis Sci* 2010;**51**:1446–52.
18. **Girkin CA**, Liebmann J, Fingeret M, *et al*. The effects of race, optic disc area, age, and disease severity on the diagnostic performance of spectral-domain optical coherence tomography. *Invest Ophthalmol Vis Sci* 2011;**52**:6148–53.
19. **Schulze A**, Lamparter J, Pfeiffer N, *et al*. Diagnostic ability of retinal ganglion cell complex, retinal nerve fiber layer, and optic nerve head measurements by Fourier-domain optical coherence tomography. *Graefes Arch Clin Exp Ophthalmol* 2011;**249**:1039–45.
20. **Hanley JA**, Hajian-Tilaki KD. Sampling variability of nonparametric estimates of the areas under receiver operating characteristic curves: an update. *Acad Radiol* 1997;**4**:49–58.
21. **R Development Core Team**. R: A Language and Environment for Statistical Computing. <http://www.R-project.org> (accessed Feb 2011).
22. **Tan O**, Li G, Lu AT, *et al*. Mapping of macular substructures with optical coherence tomography for glaucoma diagnosis. *Ophthalmology* 2008;**115**:949–56.
23. **Jeoung JW**, Park KH. Comparison of Cirrus OCT and Stratus OCT on the ability to detect localized retinal nerve fiber layer defects in preperimetric glaucoma. *Invest Ophthalmol Vis Sci* 2010;**51**:938–45.